PHYSICAL MODEL PARAMETER OPTIMISATION FOR CALIBRATED EMULATION OF THE DALLAS RANGEMASTER TREBLE BOOSTER GUITAR PEDAL

Ben Holmes and Maarten van Walstijn

Sonic Arts Research Centre,
School of Electronics, Electrical Engineering and Computer Science,
Queen's University Belfast
Belfast, U.K.
{bholmes02, mvanwalstijn}@qub.ac.uk

ABSTRACT

In this work we explore optimising parameters of a physical circuit model relative to input/output measurements, using the Dallas Rangemaster Treble Booster as a case study. A hybrid metaheuristic/gradient descent algorithm is implemented, where the initial parameter sets for the optimisation are informed by nominal values from schematics and datasheets. Sensitivity analysis is used to screen parameters, which informs a study of the optimisation algorithm against model complexity by fixing parameters. The results of the optimisation show a significant increase in the accuracy of model behaviour, but also highlight several key issues regarding the recovery of parameters.

1. INTRODUCTION

Accurate simulation of vintage audio circuits by physical modelling invariably requires the determination of component parameters. In principle, parameters can be obtained through measurement of individual components. This can present a practical dilemma though as it requires isolation and therefore deconstruction of the circuit, which particularly for vintage circuits carries hazards such as component damage. A possible way around this problem is to estimate the parameters solely from input/output (I/O) measurements, which can be taken without disassembly. Only requiring the most basic interface with a system, I/O measurements can provide significant information regarding its behaviour with relatively little effort.

The literature provides several techniques that use I/O measurements to calibrate black-box models, which have the advantage that knowledge of the actual physical component parameters is not required, and are generally designed to allow a relatively straight-forward model parameter estimation. For nonlinear systems a method of using a swept-sine to excite a system and applying an inverse filter to the output, described as 'nonlinear convolution', was proposed by Farina [1, 2]. This method was initially used for acoustic systems but was further applied to nonlinear audio circuitry in the form of Chebyshev [3] and generalised polynomial Hammerstein models [4]. Accurate modelling of the phase response is not guaranteed using this method, requiring synchronisation between input and output measurements [4, 5]. Additionally, a single set of kernels only accurately models the system at a single input level. As nonlinear systems can vary based upon amplitude it is necessary to model a continuous range of input amplitudes, which has been achieved using interpolation between sets of kernels [6].

Alleviation of these issues can be achieved using *a priori* knowledge of a system. For example, a block-oriented parametric Wiener-Hammerstein model designed specifically for distortion circuitry [7] can be said to use partial system knowledge. The partial knowledge, in this case the form of the nonlinear behaviour, constrains the identification procedure to aid in the capture of the effect's behaviour.

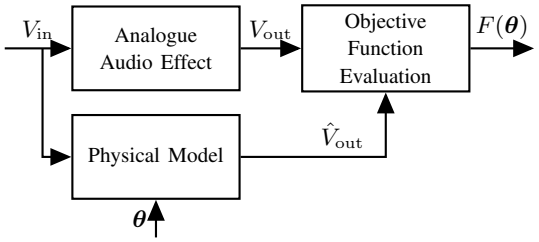

Figure 1: *Diagram illustrating the evaluation of a parameter set $\boldsymbol{\theta}$ by comparison of a physical model with said parameters and the desired analogue audio effect.*

Going a step further, physical models are based on the presumption of total knowledge of the system's behaviour. As well as accurately modelling a system's phase response and response to input amplitude (dependent upon accurate modelling of the governing physical laws), physical models can additionally capture parametric behaviour exhibited in audio effects by potentiometers, which change the behaviour of the audio effects. The two most popular physical modelling techniques, Wave Digital Filters [8] and state-space models [9], both have methods of working with parametric behaviour, with particular focus on efficiency given for state-space models [10]. However, this gain in functionality comes with a large increase in model and computational complexity. Furthermore, unlike models derived from system measurements, parameters for these models are typically extracted from nominal information available in datasheets and schematics which may not be representative of a real circuit. An exception to this strategy is when complex component models are tabulated using measurements [11]), but this requires isolation of the component.

In this paper we explore the utilisation of I/O measurements to improve the accuracy of physical models relative to specific real-world circuits. Figure 1 illustrates the evaluation of an objective function $F(\boldsymbol{\theta})$ as a measure of the fit of a physical model to a specific audio effect based upon a comparison between the circuit output voltage V_{out} and the model output voltage $\hat{V}_{\text{out}}$. The central challenge then becomes finding a parameter set that minimises the objective function for a sufficiently general excitation signal, which can be done using iterative optimisation methods. Such an approach evidently relies on the ability of the chosen physi-

cal model to capture the circuit's behaviour. An immediate further question that arises is whether a parameter set that has a low objective function value but nevertheless deviates in one or more parameters (the search space proves to typically contain many of such local minima) should be considered successful. While ideally one aims to recover the parameter set that lies closest to a physical target set, in practice (i.e. when optimising on measured results) such a target reference is not available, and the only workable criterion is the objective function. Given this lack of a direct measure of the parameter accuracy, it is proposed here that the optimisation is deemed successful if (a) the parameters lie within a physically feasible range and (b) the optimised set results in accurate model output over the relevant range of input signals and circuit potentiometer settings. The first criterion implies that the optimisation should be constrained, and the second criterion motivates performing a post-optimisation validation of the optimised parameter set using a map of driving signals of different amplitudes and frequencies within the expected input ranges.

The chosen case study for this paper is the Dallas Rangemaster Treble Booster pedal, the schematic of which is shown in Figure 2. The circuit creates a high-pass filter effect and distortion caused by the nonlinear behaviour of the germanium transistor, a Mullard OC44. The Rangemaster is a suitable initial test case for exploration of parameter optimisation of nonlinear audio effects units because despite the relative simplicity of the circuit its study fully exposes the same key challenges that can be expected in more complex systems. Three individual I/O data sets are taken of the circuit, one simulated from a stochastic parameter set, and two measured from the circuit using different transistors.

The rest of this paper is structured as follows: Section 2 discusses the selected model, details the approach used to optimise the model based on measurements, and also describes the measurement procedure. Section 3 details the application of sensitivity analysis to the model to screen the parameter set, informing a study of the performance of the optimisation algorithm with respect to increasing complexity in the model. Section 4 presents the results of the optimisation upon the I/O data sets and analyses the results using a validation data set. Sound examples are available on the first author's website[1].

2. OPTIMISATION METHOD

2.1. Circuit Description

2.1.1. Time Domain Model

A circuit can be characterised by its topology and component's behaviour. While the behaviour of two-pin linear components such as resistors and capacitors can typically be characterised with sufficient accuracy using simple laws involving a single parameter (e.g. Ohm's Law), nonlinear components such as transistors or vacuum tubes are usually modelled with several parameters. The Nodal DK-method provides a structure for automated derivation of models from this information in the form of a netlist [12], and for this reason was chosen to create the models used for the optimisation procedure. This enables direct optimisation of the parameters of the circuit as opposed to e.g. state-space matrices.

The Nodal DK-method creates a discrete-time state-space model of the form

$$\boldsymbol{x}[n] = \boldsymbol{A}\boldsymbol{x}[n-1] + \boldsymbol{B}\boldsymbol{u}[n] + \boldsymbol{C}\boldsymbol{f}(\boldsymbol{v}_{\mathrm{n}}[n]) \tag{1}$$

[1] `http://bholmesqub.github.io/DAFx16/`

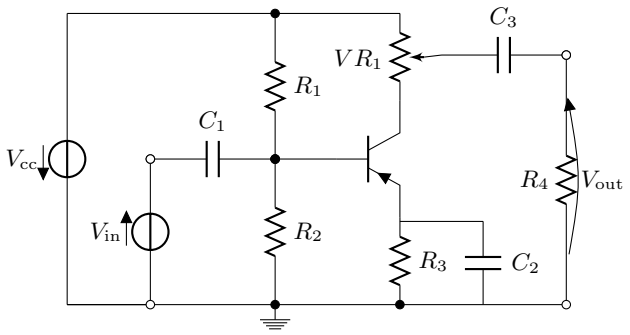

Figure 2: *Schematic of the modelled Dallas Rangemaster Treble Booster. The potentiometer VR_1, named 'Set' on the original pedal, controls the output gain or volume of the circuit.*

$$\boldsymbol{y}[n] = \boldsymbol{D}\boldsymbol{x}[n-1] + \boldsymbol{E}\boldsymbol{u}[n] + \boldsymbol{F}\boldsymbol{f}(\boldsymbol{v}_{\mathrm{n}}[n]) \tag{2}$$

$$\boldsymbol{v}_{\mathrm{n}}[n] = \boldsymbol{G}\boldsymbol{x}[n-1] + \boldsymbol{H}\boldsymbol{u}[n] + \boldsymbol{K}\boldsymbol{f}(\boldsymbol{v}_{\mathrm{n}}[n]) \tag{3}$$

where $\boldsymbol{x}$, $\boldsymbol{u}$ and $\boldsymbol{y}$ represent the state, input and output respectively, and the matrices $\boldsymbol{A} - \boldsymbol{H}$ and $\boldsymbol{K}$ specify the linear combinations that are used to update the model. The behaviour of nonlinear components is modelled by the function $\boldsymbol{f}(\boldsymbol{v}_{\mathrm{n}})$, where $\boldsymbol{v}_{\mathrm{n}}$ represents the voltages across the nonlinear components. This function is specific to the model, e.g. a model for diodes might use the Shockley diode equation. A comprehensive description of the modelling technique used can be found in [10], with the adaptation to potentiometers described in [13]. Relating this model to the Dallas Rangemaster circuit, $\boldsymbol{u}$ is the vector of the voltages $[V_{\mathrm{in}} \quad V_{\mathrm{cc}}]^{\mathrm{T}}$ applied to the circuit, and $\boldsymbol{y}$ is the modelled output voltage $\hat{V}_{\mathrm{out}}$.

It is important to note that the Dallas Rangemaster is parametric, but that the potentiometer is near equivalent to a linear scaling in output voltage. This can be inspected by testing two different models: the first with the potentiometer wiper set to 20% towards full volume, the second with the potentiometer wiper set to 100% and the output voltage scaled by 0.2. A chirp test signal between 20 Hz-3 kHz with a peak voltage of 0.2 V was processed by both models, the comparison revealing a mean squared error of 6 µV. For this reason, one measurement of the circuit with the potentiometer set at 100% is sufficiently accurate, removing the need to model the parametric behaviour.

An additional simplification is the removal of the power supply bypass capacitor, originally placed across V_{cc}. The capacitor creates a low-pass filter with the internal resistance of the power supply, which serves to smooth changes in the supplied voltage. As the focus of this paper is the usage of I/O measurements of the signal path, the supply voltage is presumed to be constant, therefore making the capacitor obsolete.

2.1.2. Bipolar Junction Transistor

To model the nonlinear behaviour of the BJT, the Ebers-Moll equations are used. This model has been widely used within the field of VA modelling [14, 10] due to its computational efficiency in comparison with more complex BJT models. The Ebers-Moll model is represented by two currents with the third being calculated using Kirchhoff's current law. Here, the base and collector currents were selected:

$$I_{\mathrm{B}} = \frac{I_{\mathrm{S}}}{\beta_{\mathrm{F}}}\left(\mathrm{e}^{\frac{V_{\mathrm{EB}}}{NV_{\mathrm{T}}}} - 1\right) + \frac{I_{\mathrm{S}}}{\beta_{\mathrm{R}}}\left(\mathrm{e}^{\frac{V_{\mathrm{EB}}-V_{\mathrm{EC}}}{NV_{\mathrm{T}}}} - 1\right) \tag{4}$$

$$I_{\mathrm{C}} = I_{\mathrm{S}}\left(\mathrm{e}^{\frac{V_{\mathrm{EB}}}{NV_{\mathrm{T}}}} - 1\right) - I_{\mathrm{S}}\frac{\beta_{\mathrm{R}}+1}{\beta_{\mathrm{R}}}\left(\mathrm{e}^{\frac{V_{\mathrm{EB}}-V_{\mathrm{EC}}}{NV_{\mathrm{T}}}} - 1\right). \quad (5)$$

The currents are controlled by the voltages of the emitter-base junction V_{EB} and the emitter-collector junction V_{EC}. The parameters are: I_{S}, the saturation current, β_{F} and β_{R}, the forward and reverse current gains, and N, the ideality factor. The ideality factor is not used in the original Ebers-Moll model [15], but is commonly included in SPICE models, and has been included in the model so that the model can match a larger range of behaviour. Temperature was not measured for this study, so the parameter N also serves to correct the value of $V_{\mathrm{T}} = 25.85\,\mathrm{mV}$, which presumes a temperature of 300 K.

2.2. Excitation Signal

Here the term excitation signal refers to the input voltage applied to the system. To expose the model to a range of frequencies, a multi-sine signal was selected, consisting of a sum of sinusoids between two frequency boundaries. This can be represented by

$$V_{\mathrm{in}}[n] = \sum_{m=m_{\mathrm{l}}}^{m_{\mathrm{u}}} A_m \sin(2\pi m f_0 nT + \phi_m) \quad (6)$$

where $f_0 = f_{\mathrm{s}}/N_{\mathrm{s}}$ and T is the sampling period $1/f_{\mathrm{s}}$. The lower and upper boundaries m_{l} and m_{u} provide a method of bandlimiting the signal, by selecting values closest to the desired lower and upper frequency boundaries. Bandlimiting is a desirable property as it enables a convenient method of focusing the measurements, for example on the expected frequency range of a guitar.

The phase terms ϕ_m are generated using Schroeder phases [16]

$$\phi_m = -2\pi \sum_{l=1}^{m-1} (m-l)A_m, \quad m = m_{\mathrm{l}}, m_{\mathrm{l}}+1, ..., m_{\mathrm{u}}. \quad (7)$$

This selection of phases distributes the sinusoids such that the peak to peak voltage is minimised, creating a flat amplitude envelope.

To determine the amplitude terms A_m, it is helpful to consider the circuit with the BJT linearised using the Hybrid Pi model [17]. The amplitude response of the linearised circuit illustrated in Figure 3 shows a significant boost to high frequencies which could prevent low frequencies from being represented in the output signal. One method of alleviating this issue is to filter the input signal using the inverse transfer function, i.e.

$$A_m = |H(j\omega_m)|^{-1}, \quad \omega_m = 2\pi m f_0 \quad (8)$$

where $|H(j\omega_m)|$ is the magnitude of the transfer function of the linearised circuit. The value of A_m is infinite at DC, but as the multi-sine signal can be band-limited, this can be managed by excluding frequencies close to DC.

Finally, to ensure that the range of voltages is sufficient, a Hann window is applied, and the signal is scaled so that the peak voltage is at 2 V. The excitation signal applied to the system has a length of 200 ms, containing frequencies between $50\,\mathrm{Hz} - 2\,\mathrm{kHz}$, as illustrated in Figure 4.

2.3. Optimisation Algorithm

Initial experiments in optimising the parameter set using a gradient descent method revealed many local minima in the search space.

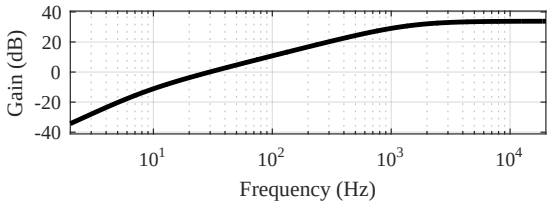

Figure 3: *Amplitude response of the linearised Dallas Rangemaster circuit.*

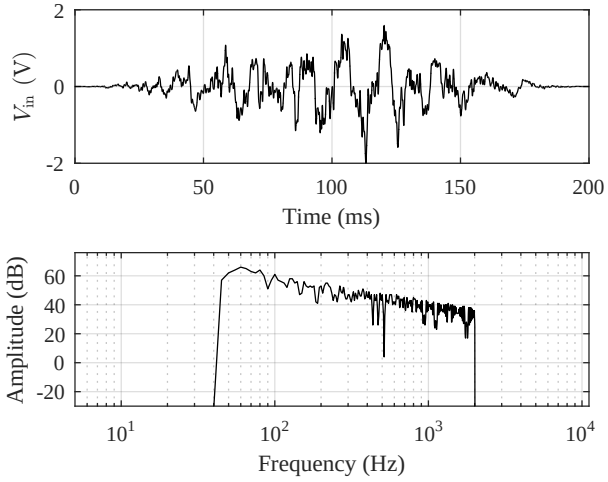

Figure 4: *Time and frequency domain representations of the excitation signal used for the I/O measurements. The ripple in the amplitude response is caused by the Hann window.*

To overcome local minima, a hybrid metaheuristic/descent method was implemented, using a Genetic Algorithm (GA) as a technique to provide a more exhaustive search. The MATLAB function `ga` provides a versatile implementation that allows the usage of floating point values as opposed to bit strings which were used in the original design of GA.

The basis of GA is to mimic principles observed in genetics and natural selection. The following description is of the MATLAB specific implementation; for a comprehensive introduction to GA see e.g. [18]. An *individual* refers to an instance of the set of parameters that characterise the model, $\boldsymbol{\theta} = [\theta_1, ..., \theta_k]^{\mathrm{T}}$ where k is the number of parameters in the set. The fitness of the individual is defined by an objective function chosen here to be of least-squares design:

$$F(\boldsymbol{\theta}) = \frac{1}{N_{\mathrm{s}}} \sum_{n=1}^{N_{\mathrm{s}}} (V_{\mathrm{out}}[n] - \hat{V}_{\mathrm{out}}[\boldsymbol{\theta}, n])^2, \quad \boldsymbol{\theta} \in \boldsymbol{\Omega} \subset \mathbb{R}^k \quad (9)$$

where V_{out} is the measured output signal, $\hat{V}_{\mathrm{out}}$ is the modelled output, and $\boldsymbol{\Omega}$ is the search space for the parameter set.

To initiate the algorithm, a *population* of individuals is randomly generated using a uniform distribution within a range of parameter values, further discussed in Section 3. The fitness value of each individual is then evaluated. A population size of 1000 individuals was chosen by increasing the size of the population until

the difference in successive generation's fitness values was negligible. Upon determining the fitness of the population, *parents* are selected to create the next generation. The most fit individuals are selected as *elites*, which are passed to the next generation without change. The remaining *children* are created from either crossover or mutation. Crossover children are created from two parents, with individual parameters selected from both parents, combined to create children. Mutation children are created from a single parent by stochastically changing parameter values. Parents are selected using a stochastic selection which helps to maintain a diverse population (i.e. a high variance of parameter values).

The implemented algorithm creates the next generation using 5% of the past population as elites, and of the remaining population 70% are generated from crossover, and 30% are generated from mutation. This process is then repeated, with the best performing parameter sets being retained while new parameter sets are generated using crossover and mutation. The main termination criterion of the algorithm is a limit of 100 generations.

A critical issue encountered when stochastically selecting parameter sets for the Dallas Rangemaster is that the simulation can fail. This happens when the nonlinear solver does not converge to the root of the equation [19]. To counteract this, failing parameter sets are regenerated using the stochastic technique used to generate the initial population. This is repeated until the simulation is successful. In addition to this, the least fit 10% of individuals are re-generated each generation to improve population diversity.

The GA algorithm is combined with the interior point method [20] which uses the top 1% of the population as starting points. This ensures that local minima are found which is not guaranteed using GA on its own. Individuals optimised with the interior point method will have a much lower fitness value than non-optimised individuals, which will cause them to be repeatedly in the top 1% of the population. As further use of the interior point method on these individuals will cause no change, they are excluded from the set which are optimised using the interior point method, and instead replaced with the next most fit individuals.

2.4. Measurement of the I/O Data Sets

Three I/O measurement data sets are used in this paper: one from a simulation using random parameters, and two measured from the Dallas Rangemaster circuit using different BJTs. The two BJTs selected for the optimisation procedure are a silicon BC557 and a germanium OC44. The OC44 is the transistor used in the original Dallas Rangemaster circuit. The BC557 is a general purpose transistor with no history of use within guitar pedals, and was selected solely for the purpose of comparison with the OC44, providing a frame of reference for the modelling of the BJT.

Measured I/O data sets used for the optimisation and sensitivity analysis were experimentally obtained from the Dallas Rangemaster circuit assembled on a breadboard. This was interfaced with MATLAB via a National Instruments ELVIS II DAQ. For the data used in the optimisation, measurements were taken at a sample rate of 100 kHz, with 100 measurements averaged to reduce noise.

A simulated I/O data set was generated to use as a comparison against the measured data. In this case there is no possibility of unmodelled behaviour, thus ensuring that the optimisation can in principle recover the parameters. This then provides a tool to assess the optimisation problem separate from problems that may be encountered with the measurements.

Table 1: *Parameters used in the modelling of the Dallas Rangemaster.*

Parameter	Value		
	Nominal	Measured	Stochastic Sample
R_1	470 kΩ	473.250 kΩ	508.209 kΩ
R_2	68 kΩ	68.596 kΩ	70.262 kΩ
R_3	3.9 kΩ	3.8965 kΩ	3.5416 kΩ
R_4	1 MΩ	0.997 MΩ	0.901 MΩ
VR_1	10 kΩ	9.999 kΩ	10.56 kΩ
C_1	4.7 nF	4.92 nF	4.44 nF
C_2	47 µF	46.95 µF	47.54 µF
C_3	10 nF	11.57 nF	9.31 nF
β_F (BC557)	340	-	-
β_F (OC44)	90	$46 - 175$	123.95
β_R (BC557)	15	-	-
β_R (OC44)	7	$2 - 12$	5.16
I_S	0.1 pA	-	0.06 pA
N	1.6	-	1.22

3. PARAMETER ANALYSIS

3.1. Determination of Parameter Values and Ranges

The first column of Table 1 shows the nominal parameters of the Dallas Rangemaster. Values for the linear parameters were extracted from the schematic. The selected optimisation algorithm allows for constraints to be placed on the range of parameters, which enables the exploitation of the tolerances specified by component manufacturers. Each value of the resistors belongs to the E12 standard which is specified at $\pm 10\%$, suggesting a sensible range with which to constrain the value of each linear component parameter. Due to the idealised component laws used in the design of the physical model, there is a possibility that the model will not capture the full behaviour of the circuit. Because of this, the linear component parameters were constrained to a range of $\pm 20\%$ to allow for compensation of the possible unmodelled behaviour. A more effective method would be to increase the complexity of the component models to capture this behaviour, but the increase in computational complexity is difficult to justify prior to observation of unmodelled behaviour. A uniform distribution was chosen for the linear component parameter set as real distributions depend on manufacturing techniques.

The BC557 values for β_F and β_R are based upon values taken from Linear Technology's LTspiceIV[2]. Datasheets and SPICE models could not be found for the OC44, so the gain parameters were measured from a small set of the BJT. The measurements were performed by applying a base current while measuring the collector current when biased in the forward-active region, and the emitter current when biased in the reverse-active region. This gives values for β_F and β_R using the approximate relations

$$\beta_\mathrm{F} \approx I_\mathrm{C}/I_\mathrm{B}, \quad \beta_\mathrm{R} \approx I_\mathrm{E}/I_\mathrm{B}.$$

Although this technique provides only a coarse approximation, it was only required to inform the range of values to be expected. The nominal values for I_S and N were set to the same value for both BJTs. The saturation current of different BJTs is often in

[2] `www.linear.com/designtools/software/#LTspice`

the same range, and is difficult to measure accurately. The ideality factor can vary widely between BJTs, particularly for vintage transistors as early manufacturing techniques provided less consistency.

Measurements of the OC44 BJT showed the range of β_{F} to be between 46 and 175, and the range of β_{R} to be between 2 and 14. Because of the wide range of these parameters, and the uncertainty of values of the parameters I_{S} and N, the BJT parameters were constrained to $\pm 100\%$ of their nominal value. A uniform distribution was again selected.

The third column of Table 1 shows the values of parameters used in the simulated data set, using BJT parameters based upon the nominal OC44 values. These were stochastically generated using the discussed uniform distributions across the parameter ranges.

3.2. Sensitivity Analysis

Global sensitivity analysis refers to the study of attributing uncertainty in a model's output to uncertainty in a model's parameters and input. The prefix 'global' specifies that the analysis is upon the whole search space as opposed to local operating points. To provide useful analysis for the optimisation, the fitness function is analysed to rank the effects of each parameter, and compare this between each I/O data set. The implemented method, the Morris method [21] generates *trajectories* through the search space using a one-at-a-time strategy i.e. there is a change in only one parameter between neighbouring sample points. An *elementary effect* of a parameter can then be defined as

$$EE_i = \frac{F(\theta_1, ..., \theta_i + \Delta, ..., \theta_k) - F(\theta_1, ..., \theta_k)}{\Delta} \tag{10}$$

where θ_i is the parameter changed by the value Δ for the elementary effect. The number of calculated elementary effects for each parameter is given by the number of trajectories, r. To prevent incorrect analysis of the sensitivity of each parameter, it is essential to select a large enough value of r. The elementary effects are processed to create two sensitivity measures, μ^* and σ expressed by

$$\mu_i^* = \frac{1}{r}\sum_{j=1}^{r}|EE_i^j|, \quad \sigma_i = \left(\frac{1}{r-1}\sum_{j=1}^{r}(EE_i^j - \mu_i)^2\right)^{\frac{1}{2}}. \tag{11}$$

The estimated absolute mean μ^* reflects the overall influence of the parameter on the fitness, and differs from the mean μ by using absolute values of the elementary effects, preventing type II errors which are caused by negative values [22]. The estimated standard deviation σ groups both the nonlinearity of the parameter and the dependence on other parameters relative to the change in the fitness function. Intuitively, this can be understood by considering a change in the value of the elementary effects: the change must either be caused by a nonlinear parameter i.e. the effect changes across the range of parameter values, or by a change in another parameter due to sampling at other locations in the space.

Analysis was performed using SAFE, a MATLAB toolbox for Global Sensitivity Analysis [23]. To help prevent any non-convergent simulations which would create unusable results, the linear component and BJT parameters were restricted to $\pm 10\%$ and $\pm 40\%$ of their nominal value respectively. A value of 300 was selected for r to ensure the search space was sufficiently analysed, although lower values or r also correctly identified the parameters with the largest and least effect on the fitness function. Figure 5 shows the results of the analysis upon the fit of the model to output measurements for the simulated, BC557, and OC44 I/O data sets. It is worth noting the near-linear relationship between μ^* and σ, indicating the parameters that have the largest effect on the fitness function are more nonlinear or heavily influenced by other parameters (i.e. parameters with high μ^* values of also have high σ values).

Parameter	Rank		
	Simulated	BC557	OC44
R_1	4	3	4
R_2	3	2	5
R_3	8	5	8
R_4	10	11	10
VR_1	5	4	6
C_1	6	8	3
C_2	9	9	9
C_3	11	12	11
I_{S}	7	6	7
N	1	1	2
β_F	2	7	1
β_R	12	10	12

Table 2: *Ranking of the circuit parameters by sensitivity value S.*

A metric for ranking parameters by their influence on the optimisation procedure was designed as $S = \sqrt{\mu^{*2} + \sigma^2}$. The rank of each parameter for each data set is shown in Table 2. Several similarities can be seen between the data sets: each fitness function is very sensitive to the parameter N and quite sensitive to both R_1 and R_2. The fitness function's low sensitivity to many of the parameters in combination with the large range of measured sensitivities indicates that the search space will contain many points with a similar fitness value; it is likely that this partly reflects a level of parameter redundancy. As a result, the optimisation may struggle to find physically meaningful parameter values.

3.3. Limitations of the Optimisation

Using the ranking of parameters of the simulated I/O data set it is possible to test the optimisation algorithm's ability to recover the values of the parameters. The performance of the algorithm can be tested against model complexity by optimising on only the N_{p} most sensitive parameters. Figure 6 displays the results of 10 optimisations performed per case for increasing values of N_{p}. The parameter error ϵ_{p} is calculated as

$$\epsilon_{\mathrm{p}} = \frac{1}{N_{\mathrm{p}}}\sum_{i=0}^{N_{\mathrm{p}}}\left(\frac{\hat{\theta}_i - \theta_i^*}{\theta_i^*}\right)^2 \tag{12}$$

where θ^* is the accurate parameter value (shown in the third column of Table 1) and $\hat{\theta}$ is the parameter value after optimisation. As the number of optimised parameters increases, the ability of the algorithm to accurately retrieve the values decreases. For the full model, the error is over 15 orders of magnitude higher than when optimising for just 2 parameters. The transition from accurately recovering parameters to failing to recover them occurs at the inclusion of the 6th parameter, C_1. After this transition the effect of the increasing quantity of parameters is negligible due to the constraints of the parameters. Given the nominal values of the

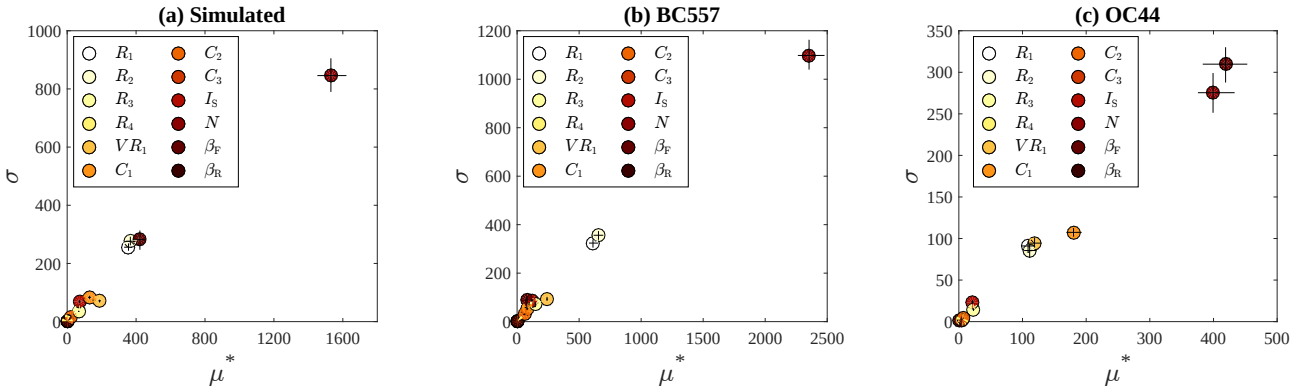

Figure 5: *Results of sensitivity analysis showing Morris measures μ^* and σ for the (a) simulated, (b) BC557, and (c) OC44 data. Confidence bounds are indicated by the black lines placed on each marker.*

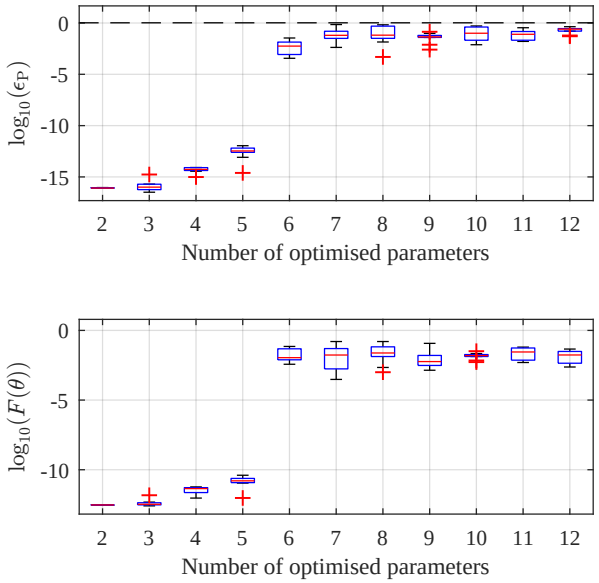

Figure 6: *Box plots displaying the logarithmic scaled error of the parameter set after optimisation on increasing numbers of optimised parameters. Red crosses indicate outliers, dashed line indicates maximum error possible with parameter constraints.*

simulated data set, the maximum parameter error is 1.0433, indicated by the dashed line on Figure 6. Results with parameter error of this order indicate that the parameters have not been recovered. The bottom plot of Figure 6 shows the log scale fitness of the resultant parameter sets from the optimisations. Although there is strong correlation with the parameter error, there is no constraint upon fitness values so this correlation cannot imply the same conclusion as with the parameter error. Fitness values of this order still provide a good fit between model and system over a wide range of operation, which can be demonstrated with the use of validation data (see Section 4).

4. RESULTS AND VALIDATION

4.1. Optimisation on the Full Parameter Set

A map of sinusoidal signals was created as a validation data set. The map covers a range of 30 peak voltages between $[0.1\,\mathrm{V}, ..., 3\,\mathrm{V}]$, and 30 frequencies between $[20\,\mathrm{Hz}, ..., 3000\,\mathrm{Hz}]$, selected logarithmically. This map was processed by both the simulation and circuit with a sample rate of $400\,\mathrm{kHz}$ to ensure that the nonlinear solver would converge. Ten measurements from the circuits were averaged to reduce noise.

Figure 7 shows the error of the model against the measurements of the validation data set. Validation error ϵ_V values were calculated using

$$\epsilon_V = 10\log_{10}\left(\sum_{n=1}^{N_s}(V_{out}[n] - \hat{V}_{out}[\hat{\boldsymbol{\theta}}, n])^2\right) \qquad (13)$$

where $\hat{\boldsymbol{\theta}}$ is the optimised parameter set. As the optimisation algorithm is stochastic, it was repeated 15 times for each I/O data set. Representative plots were selected by producing an average data map using each result, and selecting the map that closest matched this map.

The top row of the contour plots in Figure 7 shows how accurately the I/O data sets are modelled using the nominal values from Table 1. The bottom row of plots shows how accurately the I/O data sets are modelled after optimising the model parameters. The results of the simulated I/O data set illustrated in Figure 7 (a) and (d) show the results of an ideal optimisation, where there is no noise from the measurements, and the model is guaranteed to be able to represent the I/O data set. As the contour plot (d) shows, the model using the optimised parameters does accurately model the behaviour of the simulated I/O data set, but not equally well across the presented range of amplitudes and frequencies, with the most significant increase in error at higher amplitudes.

A similar increase in error is observed in Figure 7 (e) and (f), illustrating the model fit to the measured data sets of the BC557 and OC44 BJTs. Generally, the error is larger than that of the simulated data set, but significantly lower than the error of nominal parameter plots (b) and (c). This shows that despite not modelling the circuit behaviour to high accuracy, the fit is significantly better than with nominal parameters.

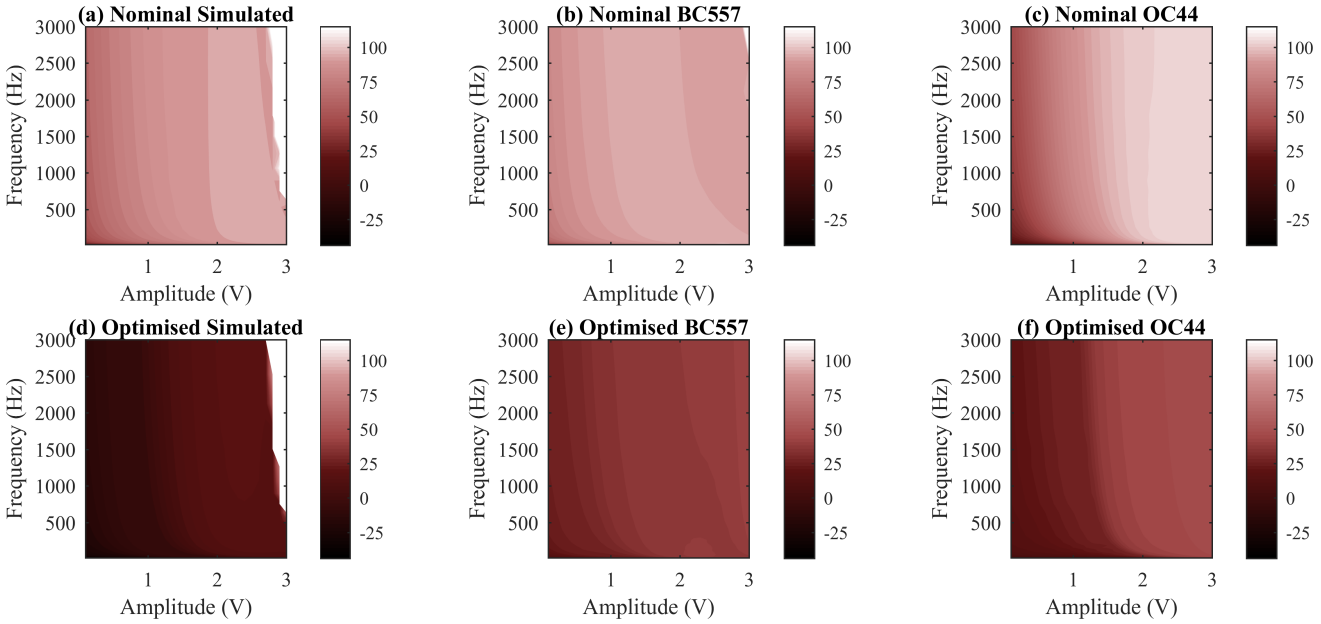

Figure 7: *Contour plots of validation error ϵ_V against amplitude (peak voltage) and frequency. White space in (a) and (d) indicates unsuccessful simulations due to nonconvergence.*

4.2. Optimisation Using Fixed Linear Component Values

To further investigate the error of the model, a second optimisation process was performed with fixed values for the linear component parameters, using the measured values shown in Table 1. This places the focus of the optimisation on the four BJT parameters used in the Ebers-Moll model. As two different BJTs were used in the measurement of the I/O data, the second optimisation aimed to investigate the performance of the Ebers-Moll model's ability to capture the behaviour of both the BC557 and OC44 BJTs. Figure 8 shows an excerpt from the output of the optimised models and the measured data they are attempting to fit. Figure 8(a) shows significantly more error than Figure 8(b), including an obvious phase difference between the model and the measurements. This points to the Ebers-Moll model not accurately capturing the behaviour of the OC44 transistor, indicating unmodelled behaviour that could be caused by e.g. junction capacitances, terminal resistances, parasitic effects etc.

5. CONCLUSION

A preliminary study on fitting a physical model of a guitar effects pedal to measured I/O data using a brute-force parameter optimisation approach has been presented. In Section 3.3 true recovery of the parameters from simulated I/O data was shown to work only for reduced sets of parameters. The results of the sensitivity analysis in Section 3.2 indicate that this could be (at least partly) due to the objective function's insensitivity to some of the parameters. It is therefore of particular interest in future research to consider alternative objective functions, alongside exploring different, even more exhaustive methods for searching the parameter space. Another possible route towards improved results regarding recovery of parameters is to consider other ways of driving the circuit and collecting the output data; potentially this includes attempts to link the physical model parameters directly to those typically used in black-box representations, (e.g. Volterra series kernel coefficients).

Although recovering the actual physical parameters proved very challenging, the results presented in Section 4 show that the accuracy of the physical model can be significantly improved using optimised instead of nominal parameters. While changes in the measurement method, objective function and optimisation (as mentioned above) can potentially further reduce the remaining errors, the results plotted in Figure 8 imply that attention must also be given to the physical model formulation. More specifically, the significantly better fit of the model to the BC557 transistor I/O data is a strong indication that the Ebers-Moll model is too simplistic to capture the behaviour of the OC44 transistor. Hence additional transistor modelling elements are required to accurately simulate the Rangemaster and other audio effects pedals and amplifiers featuring germanium BJTs. To address this, a more rigorous study of such vintage components is required, including high-accuracy measurement and subsequent comparison with more sophisticated formulations such as the Gummel-Poon model [24].

A key question to address in the longer term is to what extent models of more complex, larger circuits could be calibrated through optimisation on I/O measurement data; for systems with many more parameters than the Rangemaster it is likely that order reduction will play an even greater role, which is potentially aided by parameter screening techniques such as that employed in the present study.

6. REFERENCES

[1] A. Farina, "Simultaneous measurement of impulse response and distortion with a swept-sine technique," in *Audio En-*

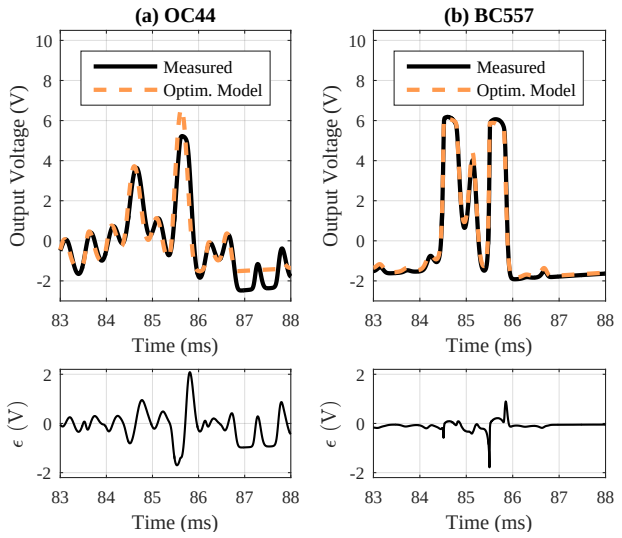

Figure 8: *Comparison of simulation output to measurement output of the Dallas Rangemaster for both the (a) OC44 and (b) BC557 circuits. The error is shown beneath each plot.*

gineering Society Convention 108. 2000, Audio Engineering Society.

[2] A. Farina, A. Bellini, and E. Armelloni, "Non-linear convolution: A new approach for the auralization of distorting systems," in *Audio Engineering Society Convention 110*. 2001, Audio Engineering Society.

[3] A. Novak, L. Simon, P. Lotton, and J. Gilbert, "Chebyshev model and synchronized swept sine method in nonlinear audio effect modeling," in *Proc. 13th Int. Conference on Digital Audio Effects*, 2010.

[4] A. Novak, L. Simon, F. Kadlec, and P. Lotton, "Nonlinear System Identification Using Exponential Swept-Sine Signal," *IEEE Transactions on Instrumentation and Measurement*, vol. 59, no. 8, pp. 2220–2229, Aug. 2010.

[5] A. Novak, P. Lotton, and L. Simon, "Synchronized Swept-Sine: Theory, Application, and Implementation," *Journal of the Audio Engineering Society*, vol. 63, no. 10, pp. 786–798, Nov. 2015.

[6] L. Tronchin and V. L. Coli, "Further Investigations in the Emulation of Nonlinear Systems with Volterra Series," *Journal of the Audio Engineering Society*, vol. 63, no. 9, pp. 671–683, Oct. 2015.

[7] F. Eichas, S. Möller, and U. Zölzer, "Block-oriented modeling of distortion audio effects using iterative minimization," in *Proceedings of the 18th International Conference on Digital Audio Effects*, Trondheim, Norway, Dec. 2015.

[8] K. J. Werner, J. O. Smith III, and J. S. Abel, "Wave digital filter adaptors for arbitrary topologies and multiport linear elements," in *Proceedings of the 18th International Conference on Digital Audio Effects*, Trondheim, Norway, Dec. 2015.

[9] M. Holters and U. Zölzer, "A generalized method for the derivation of non-linear state-space models from circuit schematics," in *23rd European Signal Processing Conference (EUSIPCO), 2015*, 2015.

[10] M. Holters and U. Zölzer, "Physical Modelling of a Wah-Wah Pedal as a Case Study for Application of the Nodal DK Method to Circuits with Variable Parts," in *Proc. of the 14th Internation Conference on Digital Audio Effects*, Paris, France, Sept. 2011.

[11] F. Eichas, M. Fink, M. Holters, and U. Zölzer, "Physical Modeling of the MXR Phase 90 Guitar Effect Pedal," in *Proc. of the 17 th Int. Conference on Digital Audio Effects*, Erlangen, Germany, Sept. 2014.

[12] D. T. Yeh, J. S. Abel, and J. O. Smith, "Automated Physical Modeling of Nonlinear Audio Circuits For Real-Time Audio Effects; Part I: Theoretical Development," *IEEE Transactions on Audio, Speech, and Language Processing*, vol. 18, no. 4, pp. 728–737, May 2010.

[13] J. Macak, J. Schimmel, and M. Holters, "Simulation of fender type guitar preamp using approximation and state-space model," in *Proceedings of the 12th International Conference on Digital Audio Effects, York, UK*, 2012.

[14] K. Dempwolf and U. Zölzer, "Discrete State-Space Model of the Fuzz-Face," in *Proceedings of Forum Acusticum*, Aalborg, Denmark, June 2011, European Acoustics Association.

[15] J. J. Ebers and J. L. Moll, "Large-signal behavior of junction transistors," *Proceedings of the IRE*, vol. 42, no. 12, pp. 1761–1772, 1954.

[16] M. Schroeder, "Synthesis of low-peak-factor signals and binary sequences with low autocorrelation (Corresp.)," *Information Theory, IEEE transactions on*, vol. 16, no. 1, pp. 85–89, 1970.

[17] R. C. Jaeger, "Small-signal models for Bipolar Junction Transistors," in *Microelectronic circuit design*. McGraw-Hill, a business unit of The McGraw-Hill Companies, Inc, New York, NY, fifth edition edition, 2015.

[18] R. L. Haupt and S. E. Haupt, *Practical genetic algorithms*, John Wiley, Hoboken, N.J, 2nd ed edition, 2004.

[19] B. Holmes and M. van Walstijn, "Improving the robustness of the iterative solver in state-space modelling of guitar distortion circuitry," in *Proceedings of the 18th International Conference on Digital Audio Effects*, Trondheim, Norway, Dec. 2015.

[20] S. P. Boyd and L. Vandenberghe, *Convex optimization*, Cambridge University Press, Cambridge, UK ; New York, 2004.

[21] M. D. Morris, "Factorial Sampling Plans for Preliminary Computational Experiments," *Technometrics*, vol. 33, no. 2, pp. 161–174, May 1991.

[22] F. Campolongo, J. Cariboni, and A. Saltelli, "An effective screening design for sensitivity analysis of large models," *Environmental Modelling & Software*, vol. 22, no. 10, pp. 1509–1518, Oct. 2007.

[23] F. Pianosi, F. Sarrazin, and T. Wagener, "A Matlab toolbox for Global Sensitivity Analysis," *Environmental Modelling & Software*, vol. 70, pp. 80–85, Aug. 2015.

[24] H. K. Gummel and H. C. Poon, "An Integral Charge Control Model of Bipolar Transistors," *Bell System Technical Journal*, vol. 49, no. 5, pp. 827–852, 1970.